Tropical peat debris storage in the tidal flat in northern part of the Bengkalis island, Indonesia

Koichi Yamamoto[1*], *Noerdin* Basir[2], *Sigit* Sutikno[3], *Ariyo* Kanno[1], *Hiroki* Kagawa[1], *Motoyuki* Suzuki[1], *Yoshihisa* Akamatsu[1], and *Atsushi* Koyama[4]

[1]Graduate School of Sciences and Technology for Innovation, Yamaguchi University, Yamaguchi, Japan
[2]Politeknik Negeri Bengkalis, Riau, Indonesia
[3]Department of Civil Engineering, Universitas Riau, Pekanbaru, Indonesia
[4]Department of Civil and Environmental Engineering, Miyazaki University, Miyazaki, Japan

Abstract. Currently, CO_2 emissions from the peat is a global problem. Particularly, it is caused by biodegradation of dry peat or peat fire. In the northern coast of Bengkalis island, peat is flowing out due to coastal erosion, and mangrove tidal flat is formed the west coast by peat. The core samples of the mangrove have been confirmed that the clay layer and the peat layer are in mutual layers, and decomposition was inhabited because these sandwiched peat soils was an anoxic state. In the northern part of the Bengkalis island, peat is sandwiched in the clay layer. Biodegradation can be suppressed by being sandwiched, there is a possibility of suppressing the amount of peat decomposed by providing a place to store peat in tidal flats. In this research, we examined the degree of decomposition of peat accumulated in the mangrove tidal flats and confirmed that decomposition was suppressed for the peat soils in the tidal flat under mangrove trees, we call it “sandwich effect”. The peat materials in deeper layer came from originally peat swamp forest, however, the surface organic materials were thought to be come from mangrove materials. Considering the change from 1988 to 2015, the carbon fixation rate by mangrove is 1.7×10^3 tC km^{-2} yr^{-1}, the carbon accumulation rate by accumulation of secondary deposition of peat was 7.4×10^3 tC km^{-2} yr^{-1}.

1 Introduction

Peat is a plant body that has accumulated undegraded as it is undecomposed, and it is also distributed in the tropics as well as high latitude region. Because peatlands generate carbon dioxide directly by biological oxidation and peat fire, conservation of the tropical peatland is a global issue [1]. The carbon dioxide emission from the peat fire on Indonesia in 1997 was comparable with the annual carbon dioxide emission from the industrial sector in the world [2]. The vertical carbon flux estimation and measurement in tropical peatland are currently mainly treated in many kinds of research because of the importance of the effect

* Corresponding author: k_yama@yamaguchi-u.ac.jp

of the oxidation of the peat, which could be affected on rising of atmospheric carbon dioxide concentration [3].

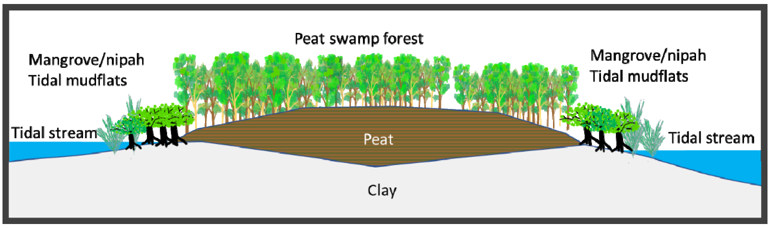

Fig. 1. Initial state of the tropical coastal peatland (after Andriesse [6]).

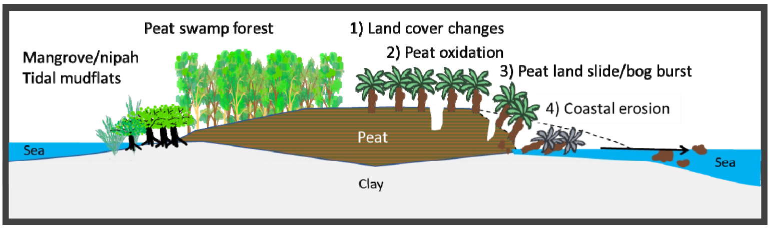

Fig. 2. Current situation of the tropical coastal peatland, especially in Riau province. Carbon fluxes are increased with several causes, such as 1) land cover changes, 2) peat oxidation, 3) peat land slide or bog burst and 4) coastal erosion.

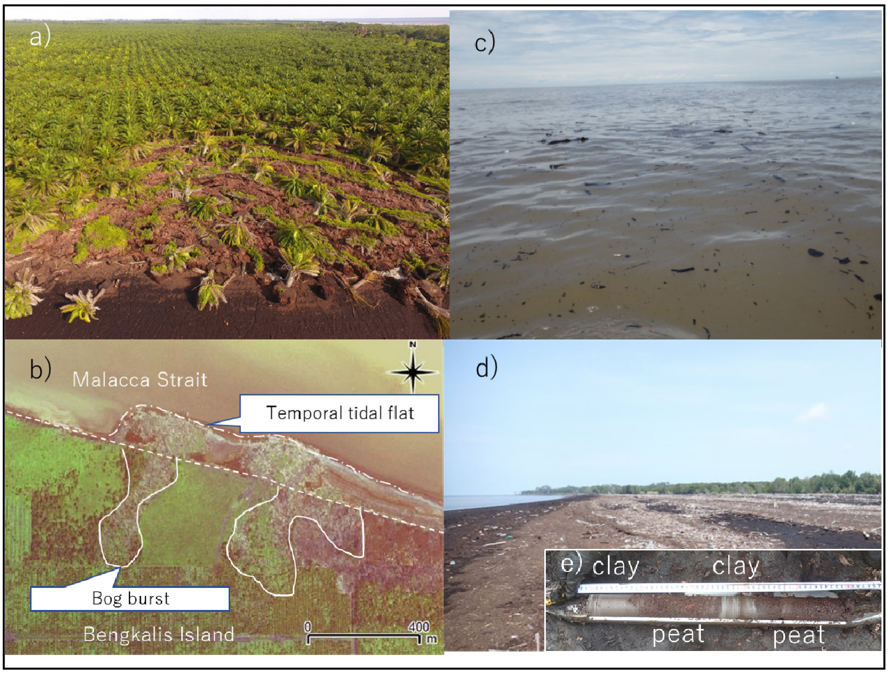

Fig. 3. Feature of the bog burst and destiny of the peat debris in tropical coastal peatland; a) Tension crack at the source zone of the bog burst (Dec. 2017, Bengkalis Island, by UAV), b) Temporal tidal flat formation by the occurrence of the bog burst (Apr. 2015, Bengkalis Island, WorldView3 satellite image), c) Floated peat debris and wood debris on the sea water of the Malacca Strait (Dec. 2017, Bengkalis Island) and d) Accumulated peat debris formed peat spit which made tidal mudflat (Aug. 2015, Bengkalis Island). e) Secondary deposited peat layers are sandwiched by clay layers (Aug. 2015, Bengkalis Island).

On the other hand, particulate organic carbon and dissolved organic carbon flux to the ocean is also necessary regarding the carbon sink into the sea floor. Global carbon export from the terrestrial biosphere is controlled by erosion [4]. Particulate organic carbon flux with the peat particle by the fluvial processes was reported [5]. However, there is no discussion of the particle organic carbon discharge by the peat coast erosion.

In the initial stage, tropical coastal peatland is fringed with mangrove [6] as shown in Fig. 1. However, the current coastal peatland has peat cliff because of the peat landslide in succession of the loss of the mangrove fringes. Peat landslides are characteristics rapid mass movements in areas dominated by organic soils [7]. Several factors affect carbon discharges from current tropical coastal peatland. Peat failure or peat landslide is one of the factors of the carbon discharges from the peatland as particle organic carbon (Fig. 2).

In the northern coast of Bengkalis Island and the Meranti Islands in Indonesia which face to the Malacca Strait, peat cliffs are formed along the coast. Also, coastal erosion is progressed rapidly. This coastal erosion is accelerated the by peat landslide which brings discharge of the peat soil into the sea, called "bog burst [7]", with making temporal tidal flat (Fig. 3(a), Fig. 3(b)). In Bengkalis Island, peat coast erosion occurred at a rate of 2.6 mm^3 per year from 2008 to 2013, with an area of 42.43 hectares per year [8].

Organic carbon that is discharged into the sea area thought to be buried in the ocean floor for a long time since it buried in the seabed [4]. However, peat debris transport in the water environment is not fully known. They will have several ways of transportation in the sea, such as flotation (Fig. 3(c)), saltation and suspension.

When the peat debris transport in floatation, they will reach shore by drifting. In northern Bengkalis island, there is peat debris fringed tidal flat (Fig. 3(d)). This peat materials are secondarily deposited, and the source of the peat debris is the peat coast situated nearby (Fig. 3(b)).

We found that the peat debris was stored in the sediment in sandwiched by the clay materials (Fig. 3(e)) in the newly formed tidal flat. If the peat particles are kept in the anaerobic status in the sediment, it will be one of the solutions of preventing emission from the carbon dioxide from the degraded coastal peatland. Anaerobic conditions in peatlands prevent the enzyme phenoloxidase from eliminating phenolic compounds that inhibit biodegradation [9]. In this research, we investigated that the degree of decomposition in the peat particles in the flat tidal sediment and peat soils in the oil palm plantation.

2 Materials and methods

2.1 Research area

Bengkalis Island lies 10 km off the coast of Sumatra along the west side of the Strait of Malacca (Fig. 4). The island is almost flat and has a maximum surface elevation of approximately 10-15 m above sea level. The area of the Island is around 900 km^2, of which 665 km^2 is covered by the peat more than 1 m thick. The whole island consists of four clay-based peat domes, the largest of which is peat in the range of about 1.5 m to 10 m altitudes with clay as the foundation. The age of the peat near the base layer is about 5000 years B.P. [10]. On the northwestern coast, clay-based peat layer of about 5 m in thickness is collapsed and facing to the Malacca Strait. Malacca strait side of the Bengkalis Island has been eroded approximately 0.5 km wide from the original peat dome state [10]. Based on the map on 1950's [11], Malacca Strait-side of the northern part of the Bengkalis Island was fringed with mangrove (F-type mangrove) at that time. However, such F-type mangrove is now degraded. Since peat swamp forest originally existed on the peat dome, logging has progressed since 2000's, and the conversion to oil palm trees progressed markedly, and waterways for the transportation of oil palm fruits and water level management for the oil palm trees growth constructed in the west part of the Bengkalis Island. In Bengkalis Island, the retreat speed of the coastline has reached 30 m per year, and erosion is still ongoing. On the other hand, mangroves are distributed on the coast of the quiet Bengkalis Strait.

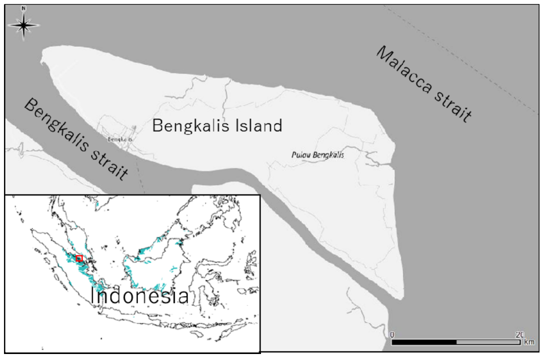

Fig. 4. Bengkalis Island (■: peatland).

2.2 Study sites

In the targeted area on the northwest edge of Bengkalis Island. Peat particles and sandbars with wood chips accumulate and tidal flats with mangroves formed behind them where the sampling stations P4–E2 are located shown in Fig. 5. Although no tidal flats were recognized at the time of the year 1988, as the coast of the northern gradually retreated, at the same time the tidal flats developed on the west coast and expanded the area. The oil palm plantation situated in the Meskom area, the northwestern part of the Bengkalis Island, where sampling stations BH1, BH2, and L1 are situated were also have chosen for the study site. The plantation has been in operation since 2001, after logging peat swamp forest. The waterway of the oil palm plantation was created as 8 meters wide and 2 meters depth to transport the oil palm bunch. We made the sampling station in the tidal flat of 7 points and 3 points in the oil palm plantation. Sampling station E3 is situated beside oil palm plantation in the peatland.

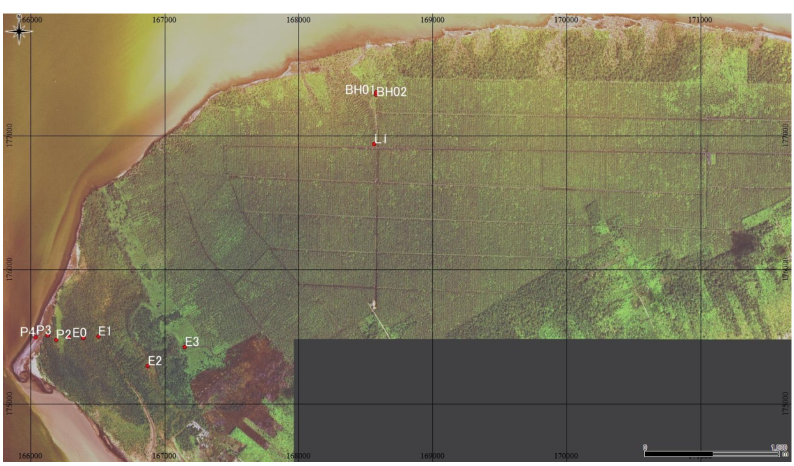

Fig. 5. Sampling stations in the northern Bengkalis Island, BH01, BH02 and L1 are situated in the oil palm plantation in the peatland, P1, P2, P3, P1, E0, E1, E2 are situated on the tidal flat. E3 is situated beside the oil palm plantation in the peatland, WorldView3 satellite image taken on Apr. 2015.

2.3 Survey method

2.3.1 Aerial photogrammetry

Aerial photogrammetry was done on September 10, 2016, for the tidal flat using quadcopter (Arris M625) with APS-C digital camera (Ricoh GR, 16.93 MP). We distributed ground control point (GCP) for aerial photogrammetry of 11 points in the tidal flat. The orange vinyl sheet of 2×2 m was used for GCPs. The coordinates of these points were measured by the geodetic GPS (Trimble 5700 and 5800). The time for the recording GNSS signal was over 15 minutes. A referenced point was Politeknik Bengkalis standard point, BM1 (N: 161378.20 m E: 182796.51 m, H: 3.26 m in UTM48N). To make a mosaic aerial photograph and to derive the 3-dimensional model of the aerial pictures, we used SfM-MVS technology [12] was used thorough Photoscan® Professional edition (Agisoft).

2.3.2 Water quality measurements

Dissolved Oxygen (DO) concentration and Oxidation Reduction Potential (ORP) were measured at point P2 in the tidal flat. Observation pipe which has the strainer of 4 cm length at 170 cm below the surface ground level. DO, and ORP sensors were set at the strainer. Measurement interval was 15 minutes, from 20th September to 25th September 2017. Groundwater table change was also measured by the measuring water pressure with HOBO U-20 Series (Onset).

2.3.3 Sampling method

Peat sampling was conducted in the oil palm plantation at BH 1 on August 19, 2014, and L1 on September 22, 2017. Sediment samples in the tidal flat were collected at P1 to P4 on August 29, E0 to E3 on September 2, 2016. Peat or sediment sampling was done using peat sampler (Eijkelkamp Soil & Water, Diameter: 50 mm). The samples were collected at vertical intervals of 25 cm from 2 to 200 cm from the ground surface and collected at intervals of 50 cm from 250 cm to 600 cm.

2.4 Chemical analysis

The collected samples were measured for moisture content, ignition loss, fiber contents (>150 um), cellulose content, and dry density and degree of humification [13] in the laboratory. Carbon and nitrogen content was measured by the combustion analysis with J-Science JM10. In the determination of the degree of humification, 0.1 g of the peat sample solute in the 10 mL of 0.025 mol L^{-1} $Na_2P_2O_7$. After shaking 18 hours in room temperature, five times dilution of the supernatant liquid was tested by the absorption of the 550 nm and 340 nm. The degree of humification was defined with 100 times of the absorbance.

2.5 Carbon storage estimation

Carbon storage amount M of the vertical average of the core at each point was calculated from equation (1) and divided by the core length to calculate the average carbon concentration in the sediment core samples from the equation (2). Next, the average carbon concentration in the transect was calculated from the equation (3). Finally, the underground organic carbon storage amount (tons) of the tideland was calculated from the equation (4). Peat deposited in the basement is thought to be sandwiched between water and clay.

Therefore, biodegradation of peat may be delayed. In other words, it can be presumed that most of the peat in the underground is stored organic carbon. Here, the carbon content (-) of layer i at point j, the carbon storage amount at point j (t m^{-2}), and the distance between the point and point. Is the depth (m) of layer i at j, the dry density (tons m^{-3}) of layer i at j, and V is the volume of newly deposited mud flats (m^3).

$$M_j = \sum_{i=1}^{n-1} \frac{c_{i,j}\rho_{d,i,j} + c_{i+1,j}\rho_{d,i+1,j}}{2}(h_{i+1,j} - h_{i,j}) \tag{1}$$

$$\overline{C_j} = \frac{M_j}{\sum_{i=1}^{n-1}(h_{i+1,j} - h_{i,j})} \tag{2}$$

$$\overline{C} = \frac{\sum_{j=1}^{m-1} \frac{\overline{C_j} + \overline{C_{j+1}}}{2}\Delta x_j}{\sum_{j=1}^{m-1}\Delta x_j} \tag{3}$$

$$M = \overline{C} \cdot V \tag{4}$$

2.6 Carbon storage estimation above the ground

In order to estimate the amount of carbon fixed by the biomass of the mangrove forest, biomass was calculated separately for the above-ground part Wu and the underground part Wb. In this study, Eq. (5) [14] was used to calculate the dry weight of branches and trunks. Also, the dry weight of root per root was calculated from Eq. (6) [15]. The relationship between tree height and breast height diameter in Eq. (7), the Spatial density of trees in Eq. (8) were obtained from the field survey. Biomass of mangroves was calculated by planar integration by Eq. (9). In mangrove trees, leaves, stems, branches, and roots of trees generally contain carbon at concentrations of 45 to 50% [16]. Therefore, the amount of carbon was calculated assuming that 50% of the dry mass of the stem, branch, and root is carbon. Here, Wu is the dry mass in the ground (kg), Wb is the dry mass in the ground (kg), D is the diameter of the breast height (m), and H is the tree height (m). a and b are coefficients. Also, is the spatial density (m^{-2}) of trees with breast height diameter D, Mtrees is the biomass (kg) of the whole area, and A is the area (m^2) of the area.

$$W_u = b\left(D^2 H\right)^a \tag{5}$$

$$W_b = 0.8069 D^{2.5154} \tag{6}$$

$$D = 0.0078H \tag{7}$$

$$\begin{aligned} \rho_{TD} &= 0.011D - 0.0152 (D \le 0.05) \\ \rho_{TD} &= -0.021D + 0.0572 (D \ge 0.06) \end{aligned} \tag{8}$$

$$M_{trees} = \int_A \rho_{TD}(W_u + W_b)dA \tag{9}$$

2.7 Estimation of the ratio of clay-derived, peat-derived, mangrove-derived organic matter

To estimate the origin of the organic matter in the collected sediment, the existence ratio was calculated by the Eq. (10) and Eq. (11) by using the end member method and *IL* of the core and organic carbon concentration.

$$\begin{pmatrix} IL_S \\ C_S \end{pmatrix} = \alpha \begin{pmatrix} IL_{Cl} \\ C_{Cl} \end{pmatrix} + \beta \begin{pmatrix} IL_P \\ C_P \end{pmatrix} + \gamma \begin{pmatrix} IL_M \\ C_M \end{pmatrix} \tag{10}$$

$$\alpha + \beta + \gamma = 1 \tag{11}$$

where α, β, γ be the abundance (-) of clay, peat and mangrove organic matter respectively, and IL_{Cl}, IL_P, IL_M be *IL* (%) of clay, peat and mangrove respectively. In addition, C_{Cl}, C_P, C_M were taken as the carbon concentration (%) of clay, peat and mangrove organic matter. Each end member is shown in Table 1.

Table 1. End members to determine the origin of the organic matter.

End members	IL (%)	C (%)	Basis of the values
Clay (*Cl*)	10	1.7	Clay layer at the sediment core sample at E3
Peat (*P*)	100	57	Averaged value of the peat layer in the core sample at E3
Mangrove organic matter (*M*)	100	30	Ratio of the C/IL of the surface sediment at E1 in Mangrove area

3 Results

3.1 Geomorphology of the new tidal flat

Digital Surface Model of the tidal flat was acquired by the photogrammetry. RMSE of the result of the photogrammetry was 0.275 m. Digital Terrain Model was derived from the interpolation by Kriging method by the extract points of no vegetation points of the DSM. The flat tidal elevation was around 0.8–1.4 m above MSL. Mean high water level around spring tide at the tidal flat in Sep. 2013 to Jan. 2014 was 1.47 m above MSL. So, the surface elevation of the top sediment was the elevation of just the sediment is covered by seawater around high tide in the spring tide. The vegetation height of the mangrove on the tidal flat was high, over 10 m high in the older tidal flat. Estimated height of the vegetation height and measured vegetation height is highly correlated (R2 = 0.9054). From P4 to P3, nipah palm and fern were dominated. From P3 to P2, Clerodendrum inerme, Ceriops tagal, Sonneratia alba sp., Rhizophora apiculate and Rhizophora mucronata were dominated. From P2 to P1, Rhizophora mucronata was dominated. Eastern part of the tidal flat was peatland, the elevation of around 3 meters.

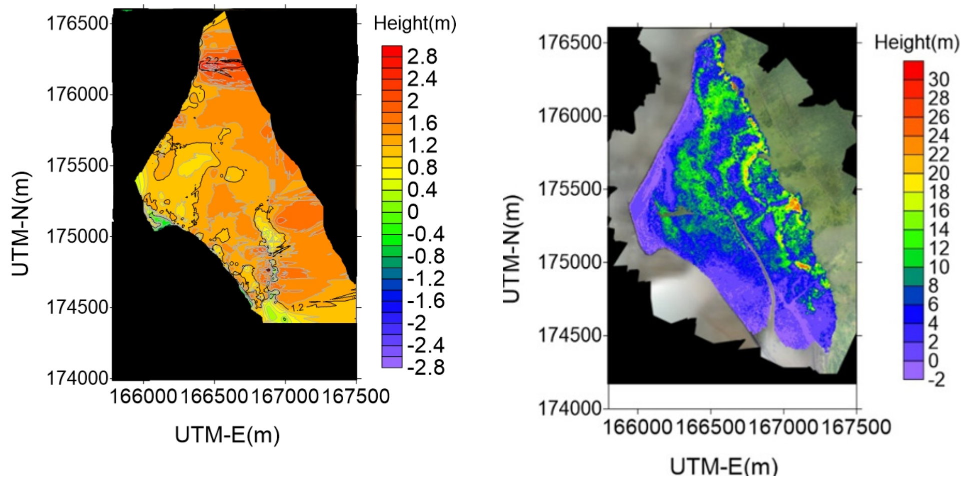

Fig. 6. Digital Terrain Model of the newly deposited tidal flat (Left) and estimated vegetation height (Right).

3.2 Eh and DO changes in the groundwater in the tidal flat

The water table of the groundwater at the strainer 1.70 m deep at measurement site P2, peat layer sandwiched with clay layers was almost stable for the measurement period (Fig. 7). Oxidation-Reduction Potential (Eh) and Dissolved Oxygen (DO) also almost stable. When the water table was above the ground level, the ground was flooded by seawater. Groundwater was maintained even when the sea water level decreased in the ebb tide. Eh has maintained around 0 mV for all the time, though there was a slight depression. DO was maintained at 0 mg/L for all the term. In anaerobic condition around 0 mV of Eh, the sulfur reduction should have happened. Methane fermentation thought to have not happened because Eh was too high for methane fermentation that happens under -200 mV of Eh. The condition of aerobic and anaerobic decomposition of the organic substances, especially the peat debris will be suppressed.

3.3 Ignition loss and degree of humification in the tidal flat sediment and peatland

Fig. 8 shows the vertical distribution of IL in the bottom sediment of the newly deposited tidal flats. Because Site E3 was completely peatland, IL was extremely high because peat was distributed more than 1 m in altitude, and its value was almost 100% (carbon concentration: 56.9%). However, IL decreased sharply from the vicinity of 1 m above the altitude, and clay content was around 10% (carbon concentration: 2%) at an altitude of 0.8 m. This was thought to be the base clay layer before peat accumulated because there was no contamination of the peat particles in the base clay layer. At all places excluding E3 point, there was a base clay layer near the altitude of -1 m. However, at an altitude of -1 m or more, IL was about 20% or more, the organic concentration was high, and peat particles were also mixed in the sediment. At the P4, P3, P2 and E1 points from the coast, peat particles were mixed, and there were some layers with extremely high organic concentration and some had IL of 50%. However, when peat particles were mixed, the dry density became low, so the average carbon content of all layers was 10%, 9.4% and 8.4% at E0 point, E1 point, E2 point, and E3 point, respectively. These sediments with high IL and carbon are not original clay but are newly deposited sediments, and some of the peat is mixed or organic matter derived from mangrove is deposited so that the carbon concentration in the sediment rises.

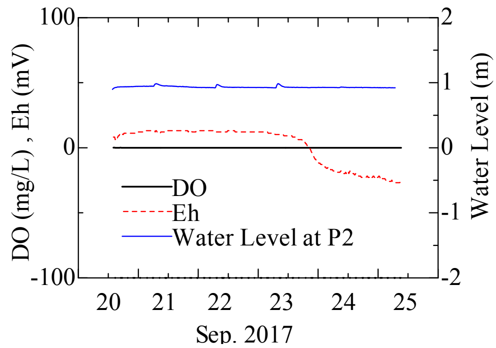

Fig. 7. Dissolved Oxygen (DO), Oxidation Reduction Potential (Eh) and ground water level of 1.7 m deep from the surface at P2, Bengkalis Island. The elevation of the ground surface was 1.0 m from MSL.

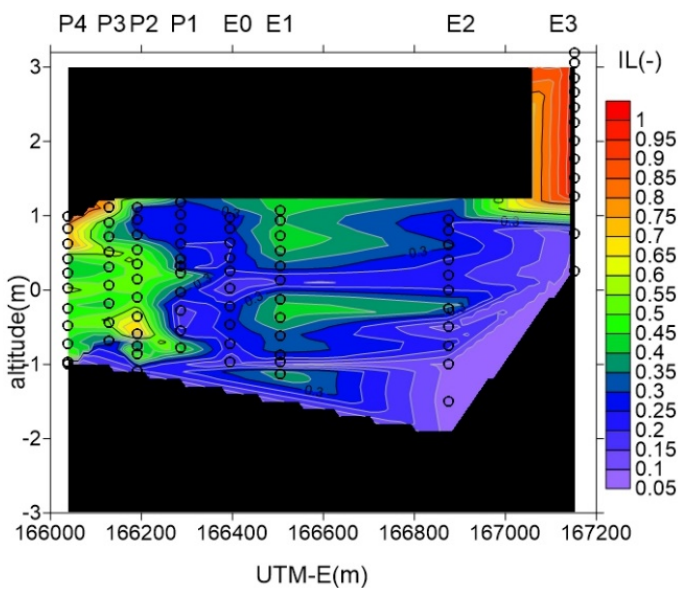

Fig. 8. Ignition loss (IL) distribution of the vertical section from P4 to E3 in the newly deposited tidal flat, shown in Fig. 5 and Fig. 6.

Fig. 9 shows the vertical two-dimensional cross-sectional distribution in the east-west direction of the degree of humus division divided by IL in order to cancel the content of inorganic matter. The degree of humification was high on the sediment surface, which was generally exposed to oxygen. It showed high values on the surface of the peatland (E3). This indicates that decomposition of peat is progressed by drying in case of peat surface. However, in the tidal area, the degree of humification was relatively lower than that of terrestrial peatlands, so it is considered that peat decomposition is suppressed or peat particles with lower humification. In Fig. 10, vertical profiles of the degree of humification in the oil palm plantation in the peatland are shown. There is the tendency that degree of humification increases above the groundwater table. Beneath the groundwater table, humification rate was almost under 150. However, over the groundwater table, degree of humification rapidly increases with the altitude. This shows that in unsaturated zone of the peat layer (*acrotelm*), decomposition of the peat materials gradually proceeds, unlike in saturated zone (*catotelm*), peat materials seem to be stable in lower decomposition rate.

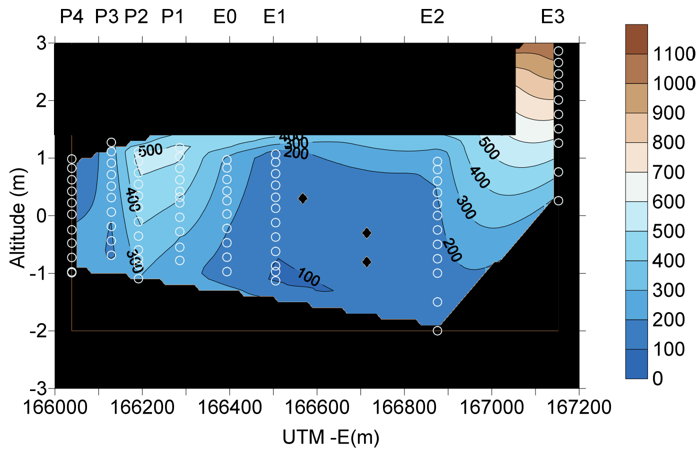

Fig. 9. Degree of humification (340 nm) distribution of the vertical section from P4 to E3 in the newly deposited tidal flat, shown in Fig. 5 and Fig. 6.

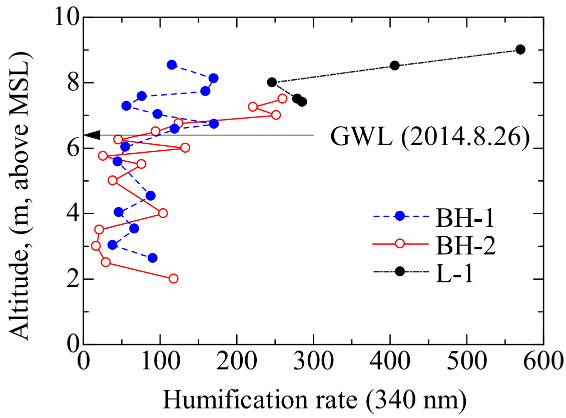

Fig. 10. Degree of humification (340 nm) profiles at BH-1, BH-2 and L-1. Groundwater level on August 26, 2014 is shown in the figure. The ground altitude of these stations of BH-1, BH-2 and L-1 were 8.5 m, 7.5 m and 9.0 m, respectively.

3.4 Amount of carbon accumulated in the newly formed tidal flat

The amount of carbon accumulated in the tidal flat is shown in Table 2. By the formation of mangrove, carbon fixed to tidal-flat for 27 years from 1988 to 2015 was 4.2×10^{2} tC km^{-2} for aboveground and carbon fixed at underground was 4.7×10^{4} tC km^{-2}. On the other hand, the amount of accumulated carbon due to the deposition of peat particles was 2.0×10^{5} tC km^{-2}.

Table 2. Storage of the organic carbon and its accumulation rate in newly formed tidal flat (Area = 1.46 km^2), Bengkalis Island, Indonesia

Term	Unit	Above ground	Underground
a) Deposited clay-derived carbon	tC km^{-2}	-	2.3×10^4
b) Deposited peat-derived carbon		-	2.0×10^5
c) Mangrove organic matter -derived carbon		-	4.5×10^4
d) Vegetation – derived carbon		4.2×10^2	2.2×10^3
e) Newly fixed carbon = c) + d)		4.2×10^2	4.7×10^4
Rate of newly fixed carbon = e) / 27 yrs	tC km^{-2} yr^{-1}	15	1.7×10^3
Rate of secondary deposition of peat = b) / 27 yrs		-	7.4×10^3

4 Conclusions

For the newly formed tidal flat beside the eroded peatland, the amount of the storage of the organic carbon in tidal flat and the degree of decomposition of the peat soils was estimated from the field survey. In the tidal flat, newly formed mangroves accumulated organic matter, and secondary deposits derived from floated peat debris that came from the other collapsed coasts were preserved and accumulated in the deep part of the tidal flat with decomposition suppressed. Peat layers were sandwiched by the clay layers. Groundwater table was maintained around the ground surface of the tidal flat. Eh and DO in the sediment were maintained around 0 mV and 0 mg/L, respectively. Such anaerobic conditions were suitable to maintain the peat particles undecomposed. By the condition of the peat layers sandwiched by clay layers, such conditions are thought to be generated. Considering the change from 1988 to 2015, the carbon fixation rate by mangrove is 1.7×10^3 tC km^{-2} yr^{-1}, the carbon accumulation rate by the accumulation of secondary deposition of peat was 7.4×10^3 tC km^{-2} yr^{-1}. Recently, coastal erosion in Riau province is severe and, there should decrease the emission of the CO_2 from the peatland by the biological decomposition. By forming tidal flat by the peat debris, peat particles will be kept in flat tidal sediment with suppressing decomposition.

This work was supported by JSPS KAKENHI Grant Number 26303015 and 17H01668.

References

1. M.R.C. Posa, L.S. Wijedasa, R.T. Corlett, Bio Science **61,**1 (2011)
2. S.E. Page, F. Siegert, J.O. Rieley, H-S.V. Boehm, A. Jaya, S. Limin, Nature **420,** 6911 (2002)
3. T. Hirano, H. Segah, K. Kusin, S. Limin, H. Takahashi, M. Osaki, Global Change Biology **18,** 11 (2012)

4. V. Galy, B. P. Ehrenbrink, T. Eglinton, Nature **521** (2015)
5. H. Marttila, B. Kløve, Journal of Hydrology **388,** 3–4 (2010)
6. J.P. Andriesse, Communication **63** (1974)
7. J.F. Shroder, *Landslide hazards, risks, and disasters* (Elsevier, New York, 2015)
8. H. Kagawa, K. Yamamoto, M. Haidar, A. Kanno, Y. Akamatsu, M. Suzuki, S. Sutikno, N. Basir, M. Sekine, J. of Japan Society of Civil Eng. **73**, 7 (2017)
9. C. Freeman, N. Otsle, H. Kang, Nature **409**, 149 (2001)
10. Supuladi, A.D. Subetky, S.G. Neuzil, Geological Society of America Special Papers **286** (1993)
11. U.S. Army Map Service, Bengkalis, Series T503, NA48-9, Available at: http://legacy.lib.utexas.edu/maps/ams/indonesia/txu-oclc-21752461-na48-9.jpg (1955)
12. N. Micheletti, J.H. Chandler, S.N. Lane, *Geomorphological techniques* (British Society, London, 2015)
13. A. Kaila, J. of the Scientific Agricultural Soc. of Finlandia **23** (1956)
14. C. Kusmana, S. Sabiham, K. Abe, H. Watanabe, Tropics **1**, 4 (1992)
15. B. Kirui, J. G. Kairo, M. Karachi, Western Indian Ocean J. of Marine Sci. **5**, 1 (2006)
16. S. Kato, Y, Sakai, T. Kojima, Bull. of the Soc. of Sea Water Sci. Japan **67** (2013)